Tohoku J. Exp. Med., 2015, **237**, 57-67

Global Gene Expression Profile of the Hippocampus in a Rat Model of Vascular Dementia

Lin Wu,[1,2,*] Xiao-Tao Feng,[1,*] Yue-Qiang Hu,[3] Nong Tang,[1,2,3] Qing-Shan Zhao,[4] Tian-Wei Li,[1] Hai-Yuan Li,[1] Qing-Bi Wang,[1] Xin-Ya Bi[1] and Xin-Kun Cai[1]

[1]Guangxi Scientific Experimental Center of Traditional Chinese Medicine, Guangxi University of Chinese Medicine, Nanning, Guangxi, P.R. China
[2]Guangxi Key Laboratory of Chinese Medicine Foundation Research, Guangxi University of Chinese Medicine, Nanning, Guangxi, P.R. China
[3]Department of Internal Neurology, The First Affiliated Hospital, Guangxi University of Chinese Medicine, Nanning, Guangxi, P.R. China
[4]Graduate School, Hunan University of Chinese Medicine, Changsha, Hunan, P.R. China

Vascular dementia (VD) has been one of the most serious public health problems worldwide. It is well known that cerebral hypoperfusion is the key pathophysiological basis of VD, but it remains unclear how global genes in hippocampus respond to cerebral ischemia-reperfusion. In this study, we aimed to reveal the global gene expression profile in the hippocampus of VD using a rat model. VD was induced by repeated occlusion of common carotid arteries followed by reperfusion. The rats with VD were characterized by deficit of memory and cognitive function and by the histopathological changes in the hippocampus, such as a reduction in the number and the size of neurons accompanied by an increase in intercellular space. Microarray analysis of global genes displayed up-regulation of 7 probesets with genes with fold change more than 1.5 ($P < 0.05$) and down-regulation of 13 probesets with genes with fold change less than 0.667 ($P < 0.05$) in the hippocampus. Gene Ontology (GO) and pathway analysis showed that the up-regulated genes are mainly involved in oxygen binding and transport, autoimmune response and inflammation, and that the down-regulated genes are related to glucose metabolism, autoimmune response and inflammation, and other biological process, related to memory and cognitive function. Thus, the abnormally expressed genes are closely related to oxygen transport, glucose metabolism, and autoimmune response. The current findings display global gene expression profile of the hippocampus in a rat model of VD, providing new insights into the molecular pathogenesis of VD.

Keywords: gene expression profile; hippocampus; ischemia-reperfusion; memory impairment; vascular dementia
Tohoku J. Exp. Med., 2015 September, **237** (1), 57-67.

Introduction

Vascular dementia (VD), an age-related chronic disease, involves the progressive loss of memory and cognitive function, accounting for nearly 20 to 40% of dementia cases after Alzheimer's disease (AD) (Lee 2011; Zhang et al. 2012a). It is reported that the prevalence of VD ranges from 0.4 to 1.6% among individuals aged 60 years and older (Lobo et al. 2000; Tiwari et al. 2013; Jia et al. 2014). Nevertheless, the prevalence still continues to rise with the rapid growth in the elderly population, thus leading to largely irreversible deterioration in patients' quality of life and increased financial burden of their families (Kalaria et al. 2008). Therefore, VD has become one of the most serious public health problems worldwide.

VD is caused by cerebrovascular diseases including stroke, hypertension, and diabetes which result in the impairment of specific brain regions involving memory and cognitive function. And the physiopathologic mechanisms of the disease are closely related to ischemia, or hemorrhagic damage, especially cerebral hypoperfusion (Decarli 2004). It is well known that hippocampus is the essential for memory and particularly vulnerable to ischemia-reperfusion (Sugawara et al. 2002; Buzsáki and Moser 2013). Ischemia-reperfusion is a complicated physiopathologic process, discontinuance and reperfusion of blood flow induces energy failure, excitatory amino acids toxicity, inflammation, oxidative stress, dysfunction of cell signaling, apoptosis, and neuronal death (White et al. 2000; Kitamura et al. 2012), which finally impair the physiologi-

Received April 27, 2015; revised and accepted August 18, 2015. Published online September 10, 2015; doi: 10.1620/tjem.237.57.
*These two authors contributed equally to this work.
Correspondence: Nong Tang, Ph.D., Guangxi Scientific Experimental Center of Traditional Chinese Medicine, Guangxi University of Chinese Medicine, 179 East Mingxiu Road, Nanning, Guangxi 530001, P.R. China.
e-mail: tangnxz2012@163.com

cal process of learning and memory. Meanwhile, the process usually results in the changes of some genes such as myelin basic protein (MBP) and monocyte chemoattractant protein-1 (MCP-1) (Kitamura et al. 2012), and the altered genes in hippocampus like insulin-like growth factor-1 (IGF-1) aggravate the process and further cause deficit of memory and cognitive function (Gong et al. 2012). However, gene expression profile in hippocampus with VD remains to be fully elucidated, which is not good for the prevention and treatment of VD.

In this study, we aimed to observe the global gene expression profile in the hippocampus of VD using a rat model. VD was induced by repeated cerebral ischemia-reperfusion, and the isolated hippocampus was used for whole genome microarray analysis. The present findings would provide new insights into the molecular pathogenesis of VD.

Materials and Methods

Animals

Male Sprague-Dawley rats, weighing 200-230 g, were purchased from Hunan Slaccas Jingda Laboratory Animal Company Limited (Changsha, China; SCXKXiang 2011-0003). The rats were maintained in a temperature- and humidity-controlled room under a 12 h light-dark cycle and had free access to food and water. All animal experiments and care were in accordance with internationally accepted principles for laboratory animal use and care and China Animal Welfare Legislation. The study was approved by the Ethics Committee of Guangxi University of Chinese Medicine. After 1 week of acclimatization, all rats were given Morris water maze test to ensure their normal memory and cognitive function.

Animal model

Rat model with VD was induced by repeated occlusion of common carotid arteries followed by reperfusion as previously described procedure with some modifications (Alipanahzadeh et al. 2014; Wu et al. 2014). Briefly, the rats were randomly divided into the sham-operated (SHAM) and the operated (OPER) groups. After anaesthesia with chloral hydrate (300 mg/kg, i.p.), bilateral common carotid arteries of the rats were exposed through a midline neck incision. Then, the arteries of rats in the operated group were ligated with 0 type surgical silk, and 0.3 ml blood was bled through tail. After 20 min, the arteries were open for 10 min by loosening the silk. This course was repeated 3 times, thus leading to cerebral ischemia-reperfusion in rats. Meanwhile, the rats in the sham-operated group were received the same surgical operation without occlusion of common carotid arteries. During the surgical procedures, the carotid sheath and vagus nerve of rats were kept from damage.

Morris water maze test

Before, after 10 and 45 days of surgery, memory and cognitive function of the rats was evaluated by the Morris water maze test according to a procedure described with some modifications (Langdon et al. 2013). The Morris water maze was made of a grey circular tank with 120 cm in diameter and 50 cm in height. The tank was divided into four quadrants and filled with water, which was maintained at 22 ± 1°C and made opaque by mixing a nontoxic water-soluble black paint. A circular platform (diameter 10 cm) was submerged about 2.0 cm below the water surface in the middle of the second quadrant. The rats were faced the sidewall of tank and released into the water to search for the hidden platform, each rat was given four trials a day (one trial for each quadrant). The time that the rats took to find the submerged platform was recorded, known as escape latency. Each rat was allowed to search for the platform within 60 s and remain on it for 10 s. When the rats could not find the platform within 60 s, they were manually directed toward the platform and allowed to remain on it for 10 s, thereby the escape latency was recorded as 60 s. Each rat was trained for 5 consecutive days. On day 6, the platform was removed, and the rats were monitored to determine whether they found the potential platform in a memory-dependent manner. The frequency that the rats passed the targeted point where the platform had been located was recorded within 60 s. The data were recorded by video and analyzed by WMT-100 Morris software (Chengdu Taimeng Software Co., Ltd., Chengdu, China). All rats were kept from a motor impairment.

Histopathological observation

Histopathology was analyzed according to the previous report with some modifications (Zhang et al. 2009). After 45 days of surgery and subsequent evaluation of memory and cognitive function, three rats in each group were randomly selected and were anesthetized with chloral hydrate (300 mg/kg, i.p.), and then perfused transcardially with normal saline followed by about 200 ml of 4% paraformaldehyde to prefix brain tissue. The brains were removed and fixed in 4% paraformaldehyde. After dehydration, the tissues were embedded with paraffin and cut into a series of sections (thickness 5 μm). The sections with hippocampus were subjected to hematoxylin and eosin (HE) staining, and the hippocampus of each rat was selected at the same layers for histological viewing.

Total RNA extraction

After 45 days of surgery and subsequent evaluation of memory and cognitive function, six rats in each group were anesthetized with chloral hydrate (300 mg/kg, i.p.) and killed by decapitation. The brain was removed, and the hippocampus was dissected. Total RNA was extracted from hippocampus and purified using Ambion mirVana miRNA Isolation Kit per the manufacture's instructions. RNA integrity was checked by agarose gel electrophoresis, and RNA purity fulfilled the following criteria: A260/280 ≥ 1.8. Then, the RNA was used in the later microarray assay.

Microarray analysis of global gene in hippocampus of rats

Microarray analysis was performed according to previously described procedure with certain modifications (Zhang et al. 2010a; Liao and Liu 2012). Briefly, RNA was used to synthesize double-stranded cDNA, and subsequently transcribed into biotin-tagged cRNA using the MessageAmp™ Premier RNA Amplification Kit (Ambion, Austin, TX). The cRNA was purified and fragmented to strands of 35-200 bases in length according to the protocols from Affymetrix. The fragmented cRNA was then hybridized to Affymetrix GeneChip® Rat Genome 230 2.0 Array containing 28, 700 transcripts, which was performed at 45°C and 60 rpm with rotation for 16 h using an Affymetrix GeneChip Hybridization Oven 640. After hybridization, the GeneChip arrays were eluted and then stained (streptavidin-phycoerythrin) on an Affymetrix Fluidics Station 450 followed by scanning on a GeneChip Scanner 3000. The scanned images were firstly assessed by visual inspection, and subsequently

analyzed using the default setting of GeneChip Operating Software (GCOS 1.4). An invariant set normalization procedure was performed to normalize the different arrays using DNA-chip analyzer (dChip). In a comparison analysis, a two-class unpaired method was used in the Significant Analysis of Microarray software (SAM) to identify significantly differentially expressed genes between the operated group and the sham-operated group. The gene, which meets a selection threshold of false discovery rate (FDR) < 5% with fold change more than 1.5 or less than 0.667, was determined to be significantly differentially expressed.

Real-time PCR confirmation

Real-time PCR was used to analyze 5 representative genes differentially expressed in the microarray. The same RNAs extracted from hippocampus samples were used. Total RNA was transcribed into cDNA. PCR reactions were carried out in an ABI 7900HT real-time PCR detection system. The protocol of real-time PCR was as follows: initial stage, 95°C for 10 min; and cycling stage, denaturation, 95°C for 15 sec, anneal and extension, 60°C for 60 sec. The sequences of primers used were: RT1-N1, forward TGC AAT TGT CCT CTG TGT TGC, reverse CTC CAT CTG CTT CCT GGG TG; Hbb, forward TGG CCT GAA ACA CTT GGA CA, reverse CCC AGG AGC CTG AAG TTC TC; RT1-CE12, forward TTG GAG CCA TCT CTG CTG TG, reverse TAG TCT CCT CCT TCC CCA CC; Pdk4, forward GGC TGA TGA CTG GTG TAT CCC, reverse CTG CCG TAG ACC CAC TTT GA; Egr2, forward TGT GCA CTG TTC TCC GAG TT, reverse TCA CAC AAG GCA CAG AGG AC; GAPDH, forward GTA CCC AGG CAT TGC TGA CA, reverse CTC CTG CTT GCT GAT CCA CAT C.

Results

Morris water maze test

In the test, there was no difference in escape latency on different training day (all $P > 0.05$, Fig. 1A) or the frequency that the rats passed the hypothetical platform ($P > 0.05$, Fig. 1B) between the operated group and the sham-operated group before surgery. But after 10 and 45 days of surgery respectively, the escape latency on different training day in the operated group was much longer than that in the sham-operated group (all $P < 0.01$, Fig. 1C, E), and the frequency in the operated group was significantly reduced when compared with the sham-operated group (all $P < 0.01$, Fig. 1D, F). The data indicate that the memory and cognitive function of rats was severely impaired by cerebral ischemia-reperfusion, suggesting that a model of VD was successfully established in rats.

Histopathological changes in hippocampus of rats

It is believed that the hippocampus is the key site for the regulation of memory and cognitive function (Takeo et al. 2003). Therefore, we observed the histopathological changes of the hippocampus. HE staining showed that the number of neurons in CA1 region of the hippocampus was decreased in the operated group, compared to the sham-operated group (Fig. 2A-D), suggesting neuronal death and loss. Indeed, the rats in the sham-operated group showed no neuronal defects or cellular changes in CA1 region of the hippocampus (Fig. 2A, B). In contrast, the neurons were arranged irregularly with increased intercellular space in the operated group. Moreover, the size of cell and nucleus was significantly decreased in the operated group, and the nucleus was unclear and underwent karyopyknosis (Fig. 2C, D). The results indicate that neurons in the hippocampus were injured by cerebral ischemia-reperfusion, further confirming the successful induction of VD in the rat.

Global gene expression profile of the hippocampus in the rat with VD

Global gene expression analysis provided insights into how gene expression in hippocampus of rats responded to cerebral ischemia-reperfusion. Microarray data were analyzed using SAM. Compared with the sham-operated group, 20 probesets with genes in the operated group were determined to be significantly differentially expressed with a threshold fold change over 1.5 or less than 0.667, including 7 up-regulated and 13 down-regulated (Table 1). The genes were visualized with TreeView tools after unsupervised hierarchical clustering (Fig. 3A). Additionally, volcano plots (Fig. 3B) were constructed based on biological and statistical significance using the microarray data from the two groups. In volcano plots, the horizontal axis shows biological impact of fold change between the two groups, based on a log scale; thus, the up-regulated genes and the down-regulated genes appear symmetric. The vertical axis represents P value, the statistical evidence, which is based on a negative log scale, suggesting that smaller P value locates higher. In Fig. 3B, green points stand for the down-regulated genes, less than 0.667 fold change with $P < 0.05$, while red points represent the up-regulated genes, more than 1.5 fold changes with $P < 0.05$.

Confirmation with real-time PCR

To confirm the microarray results, we analyzed the mRNA levels of representative genes, including Hbb, Pdk4, RT1-N1, RT1-CE12 and Egr2, by real-time PCR. As shown in Fig. 4, the relative mRNA levels of Hbb and RT1-N1 in the operated group were significantly higher, while the mRNA levels of Pdk4, RT1-CE12 and Egr2 were lower, when compared to those in the sham-operated group (all $P < 0.05$), which was consistent with the microarray results.

Gene Ontology analysis for the differentially expressed genes

To reveal the specific biological function of the differentially expressed genes, we assigned them to Gene Ontology (GO) analysis. As shown in Table 2, the genes with altered expression were divided into several large function categories. In molecular function, the genes are mainly involved in ion binding, heme binding, oxygen binding, oxygen transporter activity such as Hbb, phosphatase and kinase activity like Dusp1 and Pdk4, transcription factor activity and other molecular function. The largest category in biological process was immune response,

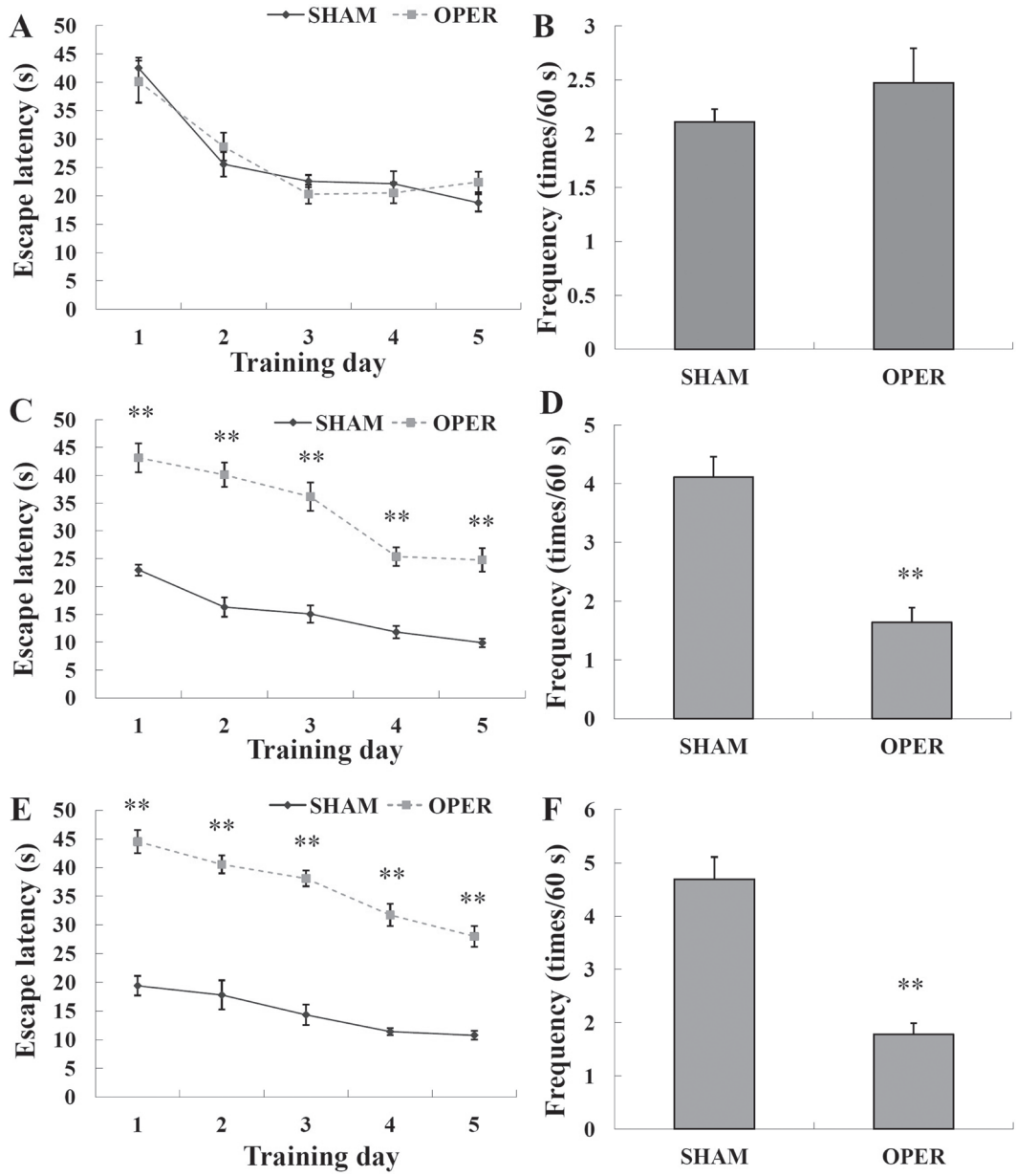

Fig. 1. Morris water maze test in the sham-operated group and the operated group. Memory and cognitive function of rats was evaluated by Morris water maze test. A. Escape latency of rats on 5 consecutive training days before surgery. B. Frequency that the rats passed the potential platform within 60 s before surgery. C. Escape latency after 10 days of surgery. D. Frequency after 10 days of surgery. E. Escape latency after 45 days of surgery. F. Frequency after 45 days of surgery. The data are presented as mean ± SE (n = 9), and significant difference between two groups was analyzed by Student's *t* test. $^{**}P < 0.01$ vs. SHAM.

including RT1-N1 and RT1-CE12 genes. Additionally, biological process still contained rhombomere formation, development, brain segmentation and Schwann cell differentiation, which have close relationship with the gene Egr2. The induced gene Pdk4 was referred to glucose metabolism. The largest category in cellular components was membrane and mitochondrion.

Pathway analysis for the differentially expressed genes

In pathway analysis (Table 3), the main pathways significantly affected in cerebral ischemia-reperfusion-induced rats were closely related to autoimmune response including graft-versus-host disease, allograft rejection, type I diabetes mellitus, autoimmune thyroid disease, antigen processing and presentation cell adhesion molecules (CAMs), which were related to RT1-N1 and RT1-CE12 genes. In addition, the gene Dusp1 was referred to MAPK signaling pathway.

Discussion

The hallmark of VD, one of the most common diseases among the old people, is progressive impairment of mem-

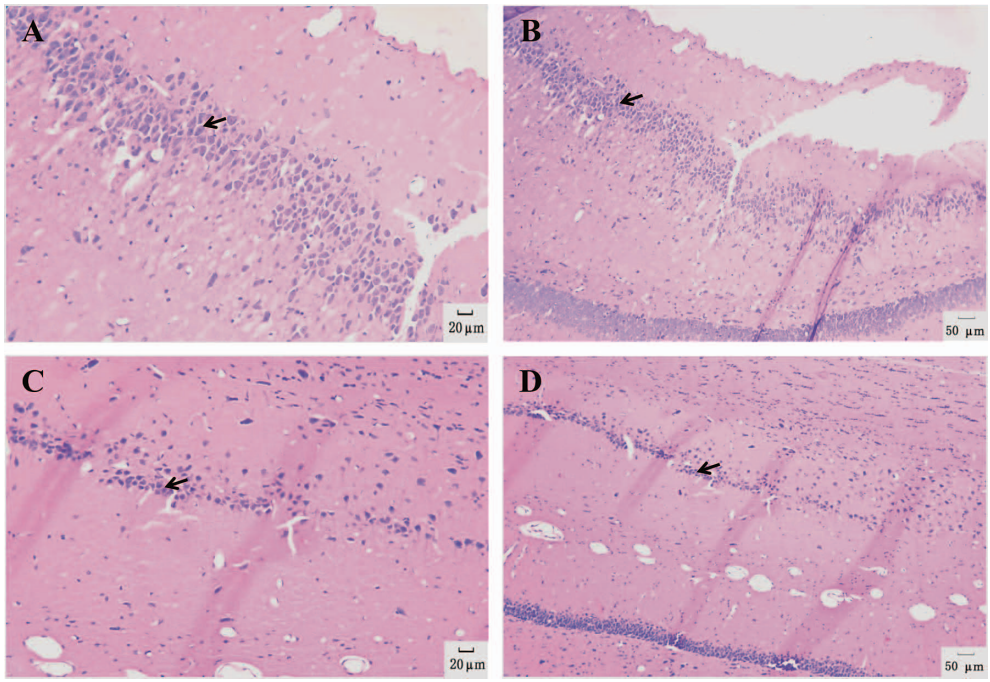

Fig. 2. Histopathological changes in hippocampus.
After 45 days of surgery and subsequent evaluation of memory and cognitive function, the brains of rats were harvested, and then subjected to HE staining. Representative photographs representing histopathology in CA1 region of hippocampus in the sham-operated group (A, scale bar, 20 μm; B, scale bar, 50 μm) and the operated group (C, scale bar, 20 μm; D, scale bar, 50 μm). The arrow indicates a representative cell with a reduced size in the operated group (C, D), when compared with a representative cell in the sham-operated group (A, B). The decrease in the number of neurons is also apparent in the CA1 region of the operated group.

ory and cognitive function because of cerebral vascular diseases. Currently, the pathogenic mechanisms of the disease have received considerable attention. Increasing evidence (de la Torre 2012; Ihara et al. 2014) indicates that cerebral hypoperfusion is the key pathophysiological basis of VD, but how global genes in hippocampus respond to cerebral ischemia-reperfusion keeps fully unclear. In this study, cerebral ischemia-reperfusion in rats was induced by repeated, transient occlusion of bilateral common carotid arteries followed by reperfusion, thus causing rats deficit of memory and cognitive function and histopathological changes in hippocampus, which was similar to the previous reports (Alipanahzadeh et al. 2014; Wu et al. 2014).

Since the hippocampus is a key site for memory and cognitive function and usually suffers from serious injury during cerebral hypoperfusion (Takeo et al. 2003; Lee et al. 2014), we analyzed the global gene expression profile of the hippocampus in the rat model using Affymetrix Gene Chip. The results showed that there were 20 differentially expressed probesets with genes in the operated group when compared with the sham-operated group, of which 7 were up-regulated and 13 were down-regulated. The data indicate that cerebral ischemia-reperfusion led to the changes of the genes, suggesting the potential molecular mechanisms of VD.

To display the biological function, we assigned the differentially expressed genes to GO and pathway analysis. Firstly, cerebral ischemia-reperfusion caused up-expression of several genes, such as Hbb and LOC100134871, related to metal ion binding, heme binding, oxygen binding, and oxygen transport. Currently, hyperbaric oxygen therapy has been used to treat VD in experimental and preliminary clinical studies (Zhang et al. 2010b; Xiao et al. 2012), but the evidence is not enough. The present study showed that repeated cerebral ischemia-reperfusion led to microvascular injury and subsequently insufficient blood supply to brain, thus resulting in aggregation of immature red blood cells in the hippocampus and up-regulated expression of Hbb and LOC100134871, which to some extent compensated for the insufficient supply of oxygen. These results provide new evidence for hyperbaric oxygen therapy in treating VD. Secondly, pyruvate dehydrogenase kinase (Pdk) family, located in mitochondria, comprise of four members (Pdk1, 2, 3, 4) and phosphorylate pyruvate dehydrogenase (PDH). Phosphorylation of PDH causes its inactivation, and vice versa (Kim et al. 2006). It is well known that pyruvate, generated from glycolysis, is converted to acetyl-CoA by PDH under normoxia, which is a critical link between glycolysis and tricarboxylic acid cycle (Kim et al. 2006), thus regulating glucose metabolism. In the present study, cerebral ischemia-reperfusion led to insufficient oxygen and glucose supply to the brain and subsequent disturbance of carbohydrate metabolism. Therefore, metabolic disturbance caused compensatory down-regulation of Pdk4 in

Table 1. The differentially expressed genes between 2 groups.

Probe Set ID	Gene Title	Gene Symbol	Fold Change
1387839_at	RT1 class Ib, locus N1 /// RT1 class Ib, locus N2	RT1-N1 /// RT1-N2	2.0885
1370658_a_at	suppression of tumorigenicity 18	St18	1.5249
1371102_x_at	hemoglobin, beta /// beta globin minor gene /// beta-globin	Hbb /// LOC100134871 /// LOC689064	1.5211
1378899_at	solute carrier family 35, member D3	Slc35d3	1.9693
1371245_a_at	beta globin minor gene /// beta-globin	LOC100134871 /// LOC689064	1.7188
1384226_at	---	---	1.8542
1389734_x_at	RT1 class I histocompatibility antigen, AA alpha chain-like /// RT1 class I, locus T24, gene 4	LOC100912480 /// RT1-T24-4	3.5677
1390813_at	Musashi homolog 2 (Drosophila)	Msi2	0.5335
1376967_at	---	---	0.4691
1388236_x_at	RT1 class I, locus CE12	RT1-CE12	0.6166
1390943_at	similar to chromosome 1 open reading frame 63	RGD1359529	0.6238
1375043_at	---	---	0.6077
1368146_at	dual specificity phosphatase 1	Dusp1	0.6213
1378074_at	pyruvate dehydrogenase kinase, isozyme 4	Pdk4	0.6033
1371033_at	similar to RT1 class II histocompatibility antigen, B-1 beta chain precursor (RT1.B-beta(1)) /// RT1 class II, locus Bb	LOC688090 /// RT1-Bb	0.4959
1388202_at	RT1 class Ib, locus EC2	RT1-EC2	0.2006
1388203_x_at	RT1 class I, locus CE11-like /// RT1 class I, locus A3 /// RT1 class I, locus CE10 /// RT1 class I, locus CE2 /// RT1 class Ib, locus EC2	LOC100364500 /// RT1-A3 /// RT1-CE10 /// RT1-CE2 /// RT1-EC2	0.2697
1382712_at	---	---	0.6402
1387306_a_at	early growth response 2	Egr2	0.5678
1388506_at	desmoplakin	Dsp	0.647

rats with cerebral ischemia-reperfusion, which released the inhibition of PDH activity by Pdk4 and partially promoted carbohydrate metabolism. The data mean improving glucose and energy metabolism may be an important strategy for the treatment of VD. Thirdly, a growing body of evidence (Zuliani et al. 2007a, b; Zhang et al. 2012b) indicates that plasma cytokines such as TNF-α and IL-1β in VD patients and hippocampal inflammatory factors in VD rats are increased, and that inhibiting inflammatory response improves cognitive impairment in VD rats, implying inflammatory status influences the onset of VD. Moreover, VD is often associated with increased autoantibodies (Mosek et al. 2000; de Godoy et al. 2005). In the present study, GO and pathway analysis showed that both of differentially expressed genes RT1-N1 and RT1-CE12 had close relationship with autoimmune response. In this context, immune system activation exerts a remarkable role in the development and progression of neurodegenerative disorders (Malaguarnera et al. 2006).

The brain is an immunologically privileged site because of blood-brain barrier (BBB), which blocks the entry of macromolecules into the brain, such as immunoglobulins (Ig) and cells, including the immunocompetent ones, thus protecting and isolating brain from organism's immune reaction. If the integrity of BBB is destroyed by microvascular injury or inflammation, increasing amounts of immunocompetent macromolecules and cells including T and B cells will pass BBB into the brain, especially hippocampus, and then cause increased expression of major histocompatibility complex (MHC) I and II in endothelial cells and glia cells, thus triggering subsequent autoimmune response (Mattila et al. 1994; Sardi et al. 2011). Under physiological conditions, synaptic connected proteins are not recognized by immune system cells. However, once cerebral ischemia-reperfusion injured BBB, the primary and new connected proteins are recognized by immune system cells, which lead to autoimmune response and subsequent secretion of inflammatory factors from activated immune cells (Arshavsky 2006; Sardi et al. 2011). RT1-N1 referred to the class I major histocompatibility and was responsible for antigen processing and presentation, the key step of triggering autoimmune response. Here, RT1-N1 was up-regu-

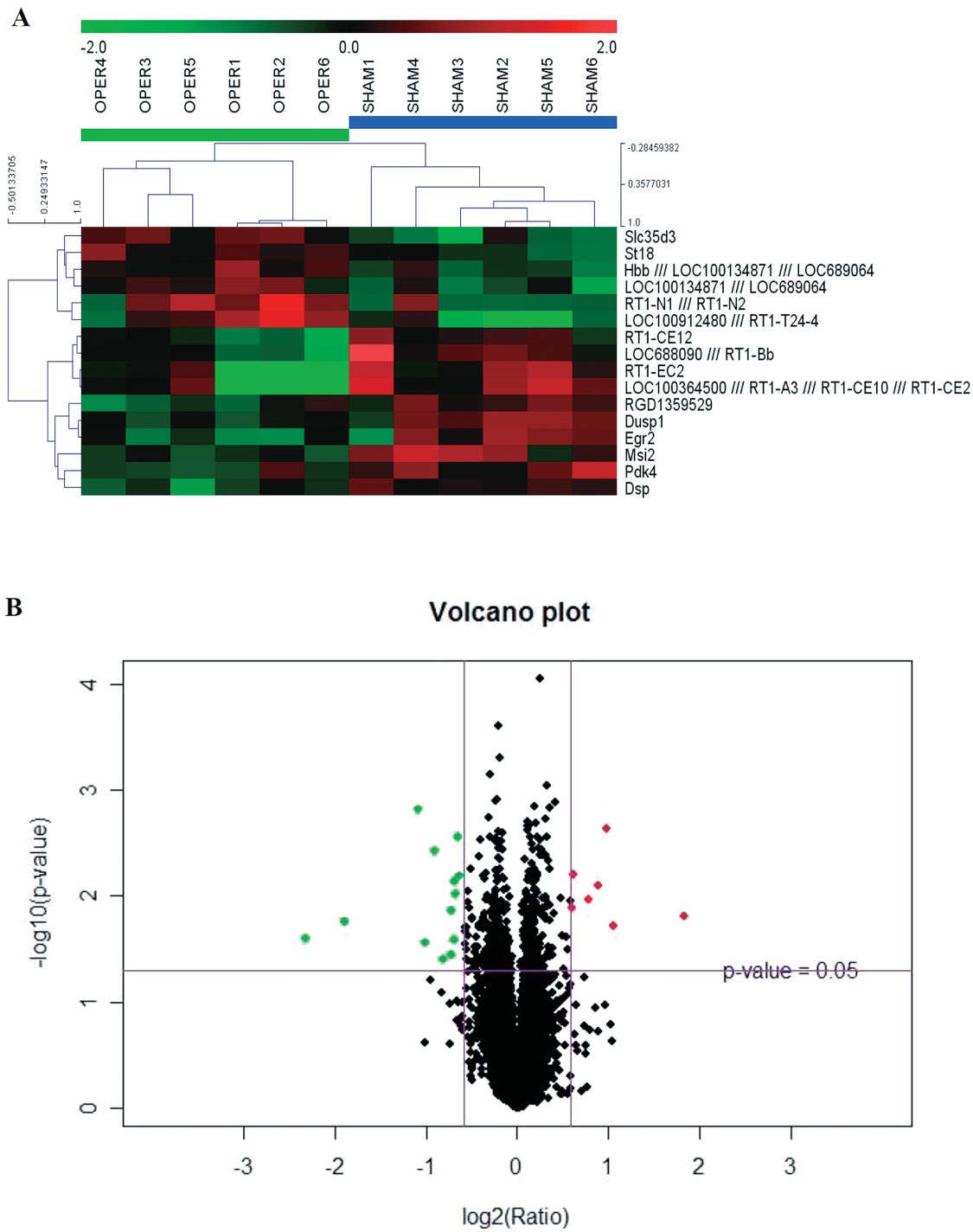

Fig. 3. Clustering display of microarray data and volcano plots.
A. The differentially expressed genes between the operated group (n = 6) and the sham-operated group (n = 6) were performed using SAM software and visualized with TreeView tools upon hierarchical clustering. Gene symbols are labeled on the right. A color tag represents gene expression level, red spectrum denotes up-regulated genes, and green for down-regulated ones. B. Volcano plot displayed the differentially expressed genes between the operated group and the sham-operated group. The horizontal axis shows the change of fold, and the vertical indicates the statistical significance. Green points represent the down-regulated genes with fold change less than 0.667 and $P < 0.05$, red points denote the up-regulated genes with fold change more than 1.5 and $P < 0.05$.

lated in hippocampus of VD rats, and immune system activation induced production of inflammatory factors, which penetrated BBB and further cause cognitive impairment. One report showed that tacrolimus (FK506), an immunosuppressant, ameliorates learning impairment in rats with chronic cerebral hypoperfusion (Tanaka et al. 2001). The

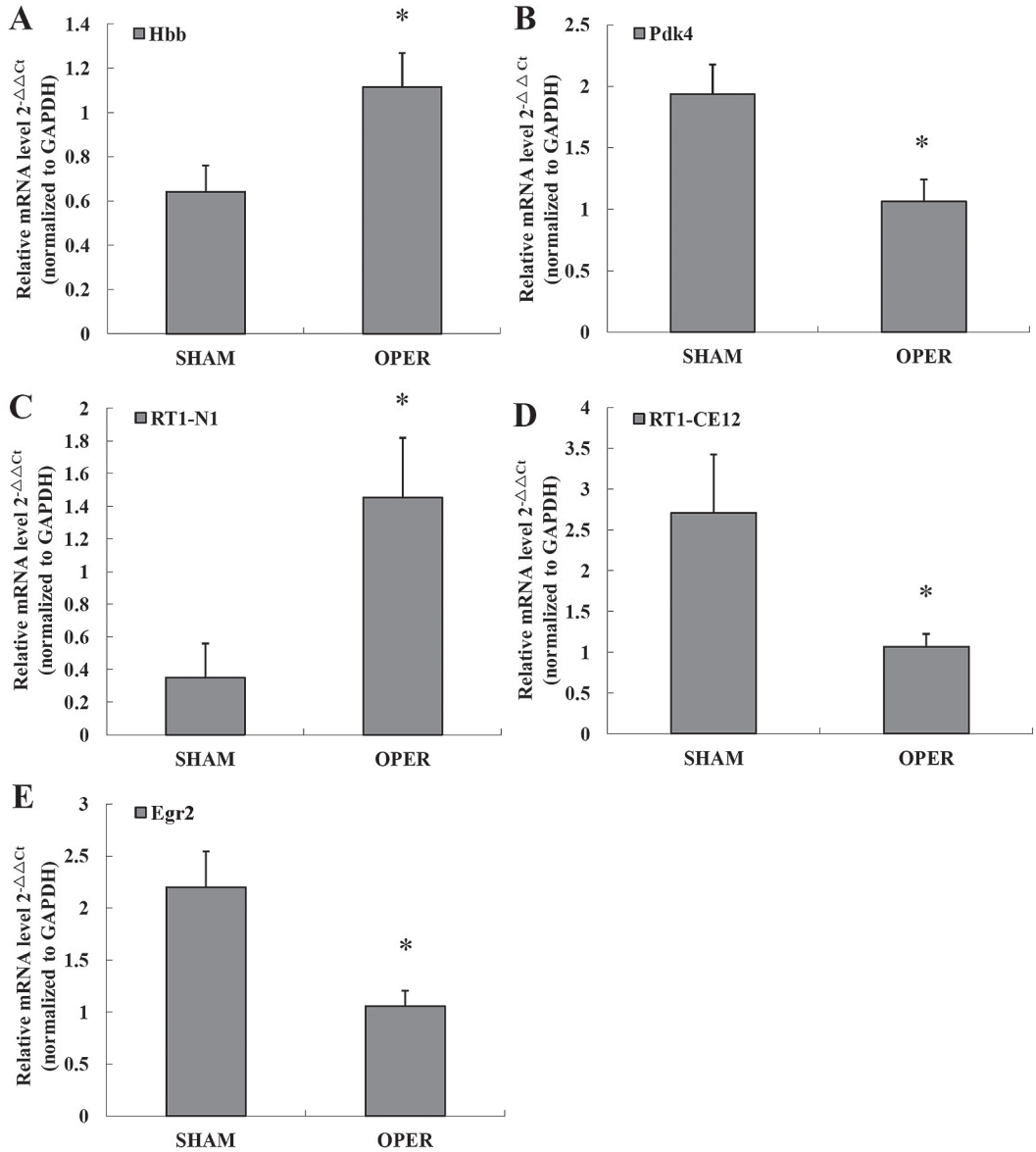

Fig. 4. The relative mRNA levels of 5 differentially expressed genes.
The mRNA levels of Hbb (A), Pdk4 (B), RT1-N1 (C), RT1-CE12 (D) and Egr2 (E) were quantified by Real-time PCR to confirm the microarray results. The data are presented as mean ± SE, and significant difference between two groups was analyzed by Student's *t* test. **P* < 0.05, vs. SHAM.

data in the study demonstrate that autoimmune mediation is likely an important part of the disease process.

Additionally, it is well known that both of late phase long-term potentiation (LTP) and consolidation of long-lasting memories have a common mechanism that triggers activation of immediate early genes (IEGs). The family of early growth response genes (Egr), containing four members, Egr1, 2, 3, and 4, belong to IEGs that encode transcription factors. Studies reveal that learning and retrieval promote Egr1 translation and lead to an increase in binding of constitutively expressed Egr1 to the Egr response element (ERE) (Cheval et al. 2012). Moreover, Egr1 plays a crucial role in memory formation through regulating synaptic transport, synaptic transmission (Koldamova et al. 2014), and synaptic plasticity. Since having similar protein structure, Egr2 maybe shares similar function with Egr1. In fact, memory recall is accompanied by increased Egr2 mRNA expression, specific role of Egr2-mediated transcriptional activation in cognitive functions associates with attention (DeSteno and Schmauss 2008). In the present study, cerebral ischemia-reperfusion caused down-expression of Egr2 with impaired memory and cognitive function, and GO analysis showed Egr2 associated with myelination, Schwann cell differentiation, brain segmentation and other biological process, consistent with the previous report (DeSteno and Schmauss 2008).

Together, the current data indicate that repeated cerebral ischemia-reperfusion resulted in impairment of mem-

Table 2. Gene ontology classification for the differentially expressed genes.

GO Term	Count	Input Symbol	*P* Value
Molecular function			
GO:0005344 oxygen transporter activity	2	Hbb; LOC100134871	8.78E-07
GO:0019825 oxygen binding	2	Hbb; LOC100134871	5.02E-06
GO:0031721 hemoglobin alpha binding	1	Hbb	1.20E-04
GO:0031722 hemoglobin beta binding	1	Hbb	1.20E-04
GO:0020037 heme binding	2	Hbb; LOC100134871	5.58E-04
GO:0046872 metal ion binding	4	St18; Hbb; LOC100134871; Egr2	0.002276341
GO:0017017 MAP kinase phosphatase activity	1	Dusp1	0.001435633
GO:0004725 protein tyrosine phosphatase activity	1	Dusp1	0.017337393
GO:0000155 two-component sensor activity	1	Pdk4	0.001794243
GO:0004740 [pyruvate dehydrogenase (lipoamide)] kinase activity	1	Pdk4	3.59E-04
GO:0003700 transcription factor activity	2	St18; Egr2	0.007228532
GO:0008270 zinc ion binding	2	St18; Egr2	0.047460321
Biological process			
GO:0006955 immune response	3	RT1-N1; RT1-CE12; LOC688090	4.84E-07
GO:0019882 antigen processing and presentation	2	RT1-N1; RT1-CE12	2.29E-06
GO:0002504 antigen processing and presentation of peptide or polysaccharide antigen via MHC class II	1	LOC688090	0.002630532
GO:0002474 antigen processing and presentation of peptide antigen via MHC class I	1	RT1-CE12	0.006326287
GO:0021660 rhombomere 3 formation	1	Egr2	1.20E-04
GO:0021666 rhombomere 5 formation	1	Egr2	1.20E-04
GO:0021569 rhombomere 3 development	1	Egr2	3.59E-04
GO:0021612 facial nerve structural organization	1	Egr2	3.59E-04
GO:0035284 brain segmentation	1	Egr2	3.59E-04
GO:0014037 Schwann cell differentiation	1	Egr2	8.38E-04
GO:0008045 motor axon guidance	1	Egr2	0.001076905
GO:0007622 rhythmic behavior	1	Egr2	0.001555183
GO:0042552 myelination	1	Egr2	0.004062658
GO:0045944 positive regulation of transcription from RNA polymerase II promoter	1	Egr2	0.019220315
GO:0030278 regulation of ossification	1	Egr2	0.005731059
GO:0001503 ossification	1	Dsp	0.01308854
GO:0042060 wound healing	1	Dsp	0.017101792
GO:0006470 protein amino acid dephosphorylation	1	Dusp1	0.019572989
GO:0006355 regulation of transcription, DNA-dependent	2	St18; Egr2	0.021926887
GO:0006006 glucose metabolism	1	Pdk4	0.041555588
GO:0006086 acetyl-CoA biosynthesis from pyruvate	1	Pdk4	5.98E-04
GO:0018106 peptidyl-histidine phosphorylation	1	Pdk4	8.38E-04
GO:0015671 oxygen transport	2	Hbb; LOC100134871	1.40E-06
GO:0051291 protein heterooligomerization	1	Hbb	0.005016348
Cellular component			
GO:0042612 MHC class I protein complex	2	RT1-N1; RT1-CE12	6.73E-07
GO:0042613 MHC class II protein complex	1	LOC688090	0.002988743
GO:0016020 membrane	3	RT1-N1; RT1-CE12; LOC688090	0.014751915
GO:0005916 fascia adherens	1	Dsp	2.39E-04
GO:0030057 desmosome	1	Dsp	3.59E-04
GO:0005739 mitochondrion	2	Pdk4; Dsp	0.003929688
GO:0005759 mitochondrial matrix	1	Pdk4	0.012142037
GO:0005743 mitochondrial inner membrane	1	Pdk4	0.030563993
GO:0005833 hemoglobin complex	2	Hbb; LOC100134871	5.98E-07
GO:0016323 basolateral plasma membrane	1	Dsp	0.012615394
GO:0005578 extracellular matrix (sensu Metazoa)	1	Dsp	0.031842669

Items were listed here when P value < 0.05.

Table 3. Pathway classification for the differentially expressed genes.

Pathway	Count	Gene	*P* Value
Graft-versus-host disease	2	RT1-N1; RT1-CE12	8.97E-05
Allograft rejection	2	RT1-N1; RT1-CE12	9.59E-05
Type I diabetes mellitus	2	RT1-N1; RT1-CE12	1.19E-04
Autoimmune thyroid disease	2	RT1-N1; RT1-CE12	1.23E-04
Antigen processing and presentation	2	RT1-N1; RT1-CE12	2.63E-04
Natural killer cell mediated cytotoxicity	2	RT1-N1; RT1-CE12	5.19E-04
Cell adhesion molecules (CAMs)	2	RT1-N1; RT1-CE12	5.79E-04
MAPK signaling pathway	1	Dusp1	0.061623951

ory and cognitive function in rats, and caused up-regulation of 7 probesets with genes and down-regulation of 13 probesets with genes, involving oxygen transport, glucose metabolism, and autoimmune response, which provide new insights into the molecular pathogenesis of VD.

Acknowledgments

This work was supported by the National Natural Science Foundation of China (No. 81160435), Guangxi Department of Health (No. GZKZ-Z1102), and Guangxi Key Laboratory of Chinese Medicine Foundation Research (Nos. 14-045-42 and 13-051-35), Guangxi University of Chinese Medicine. Microarray analysis of global genes was performed in the National Engineering Research Center for Beijing Biochip Technology (Beijing CapitalBio Corporation, China).

Author Contributions

Nong Tang was responsible for study design and revised the manuscript. Lin Wu and Xiao-Tao Feng conducted the research and statistical data, and wrote the manuscript. Yue-Qiang Hu provided technical assistance during the experiments. Other authors performed the experiments and collected data.

Conflict of Interest

The authors declare no conflict of interest.

References

Alipanahzadeh, H., Soleimani, M., Soleimani Asl, S., Pourheydar, B., Nikkhah, A. & Mehdizadeh, M. (2014) Transforming growth factor-α improves memory impairment and neurogenesis following ischemia reperfusion. *Cell J.*, **16**, 315-324.

Arshavsky, Y.I. (2006) Alzheimer's disease, brain immune privilege and memory: a hypothesis. *J. Neural. Transm.*, **113**, 1697-1707.

Buzsáki, G. & Moser, E.I. (2013) Memory, navigation and theta rhythm in the hippocampal-entorhinal system. *Nat. Neurosci.*, **16**, 130-138.

Cheval, H., Chagneau, C., Levasseur, G., Veyrac, A., Faucon-Biguet, N., Laroche, S. & Davis, S. (2012) Distinctive features of Egr transcription factor regulation and DNA binding activity in CA1 of the hippocampus in synaptic plasticity and consolidation and reconsolidation of fear memory. *Hippocampus*, **22**, 631-642.

Decarli, C. (2004) Vascular factors in dementia: an overview. *J. Neurol. Sci.*, **226**, 19-23.

de Godoy, J.M., de Godoy, M.R., Cipulo, J.P. & Tognola, V.A. (2005) Vascular dementia and anticardiolipin antibodies. *Med. Sci. Monit.*, **11**, CR430-CR433.

de la Torre, J.C. (2012) Cardiovascular risk factors promote brain hypoperfusion leading to cognitive decline and dementia. *Cardiovasc. Psychiatry Neurol.*, **2012**, 367516.

DeSteno, D.A. & Schmauss, C. (2008) Induction of early growth response gene 2 expression in the forebrain of mice performing an attention-set-shifting task. *Neuroscience*, **152**, 417-428.

Gong, X., Ma, M., Fan, X., Li, M., Liu, Q., Liu, X. & Xu, G. (2012) Down-regulation of IGF-1/IGF-1R in hippocampus of rats with vascular dementia. *Neurosci. Lett.*, **513**, 20-24.

Ihara, M., Taguchi, A., Maki, T., Washida, K. & Tomimoto, H. (2014) A mouse model of chronic cerebral hypoperfusion characterizing features of vascular cognitive impairment. *Methods Mol. Biol.*, **1135**, 95-102.

Jia, J., Wang, F., Wei, C., Zhou, A., Jia, X., Li, F., Tang, M., Chu, L., Zhou, Y., Zhou, C., Cui, Y., Wang, Q., Wang, W., Yin, P., Hu, N., et al. (2014) The prevalence of dementia in urban and rural areas of China. *Alzheimers Dement.*, **10**, 1-9.

Kalaria, R.N., Maestre, G.E., Arizaga, R., Friedland, R.P., Galasko, D., Hall, K., Luchsinger, J.A., Ogunniyi, A., Perry, E.K., Potocnik, F., Prince, M., Stewart, R., Wimo, A., Zhang, Z.X., Antuono, P., et al. (2008) Alzheimer's disease and vascular dementia in developing countries: prevalence, management, and risk factors. *Lancet Neurol.*, **7**, 812-826.

Kim, J.W., Tchernyshyov, I., Semenza, G.L. & Dang, C.V. (2006) HIF-1-mediated expression of pyruvate dehydrogenase kinase: a metabolic switch required for cellular adaptation to hypoxia. *Cell Metab.*, **3**, 177-185.

Kitamura, A., Fujita, Y., Oishi, N., Kalaria, R.N., Washida, K., Maki, T., Okamoto, Y., Hase, Y., Yamada, M., Takahashi, J., Ito, H., Tomimoto, H., Fukuyama, H., Takahashi, R. & Ihara, M. (2012) Selective white matter abnormalities in a novel rat model of vascular dementia. *Neurobiol. Aging*, **33**, 1012. e25-35.

Koldamova, R., Schug, J., Lefterova, M., Cronican, A.A., Fitz, N.F., Davenport, F.A., Carter, A., Castranio, E.L. & Lefterov, I. (2014) Genome-wide approaches reveal EGR1-controlled regulatory networks associated with neurodegeneration. *Neurobiol. Dis.*, **63**, 107-114.

Langdon, K.D., Granter-Button, S., Harley, C.W., Moody-Corbett, F., Peeling, J. & Corbett, D. (2013) Cognitive rehabilitation

reduces cognitive impairment and normalizes hippocampal CA1 architecture in a rat model of vascular dementia. *J. Cereb. Blood Flow Metab.*, **33**, 872-879.

Lee, A.Y. (2011) Vascular dementia. *Chonnam Med. J.*, **47**, 66-71.

Lee, J.Y., Lee, H.E., Kang, S.R., Choi, H.Y., Ryu, J.H. & Yune, T.Y. (2014) Fluoxetine inhibits transient global ischemia-induced hippocampal neuronal death and memory impairment by preventing blood-brain barrier disruption. *Neuropharmacology*, **79**, 161-171.

Liao, M. & Liu, H. (2012) Gene expression profiling of nephrotoxicity from copper nanoparticles in rats after repeated oral administration. *Environ. Toxicol. Pharmacol.*, **34**, 67-80.

Lobo, A., Launer, L.J., Fratiglioni, L., Andersen, K., Di Carlo, A., Breteler, M.M., Copeland, J.R., Dartigues, J.F., Jagger, C., Martinez-Lage, J., Soininen, H. & Hofman, A. (2000) Prevalence of dementia and major subtypes in Europe: A collaborative study of population-based cohorts. Neurologic Diseases in the Elderly Research Group. *Neurology*, **54**, S4-S9.

Malaguarnera, L., Motta, M., Di Rosa, M., Anzaldi, M. & Malaguarnera, M. (2006) Interleukin-18 and transforming growth factor-beta 1 plasma levels in Alzheimer's disease and vascular dementia. *Neuropathology*, **26**, 307-312.

Mattila, K.M., Pirttila, T., Blennow, K., Wallin, A., Viitanen, M. & Frey, H. (1994) Altered blood-brain-barrier function in Alzheimer's disease? *Acta Neurol. Scand.*, **89**, 192-198.

Mosek, A., Yust, I., Treves, T.A., Vardinon, N., Korczyn, A.D. & Chapman, J. (2000) Dementia and antiphospholipid antibodies. *Dement. Geriatr. Cogn. Disord.*, **11**, 36-38.

Sardi, F., Fassina, L., Venturini, L., Inguscio, M., Guerriero, F., Rolfo, E. & Ricevuti, G. (2011) Alzheimer's disease, autoimmunity and inflammation. The good, the bad and the ugly. *Autoimmun. Rev.*, **11**, 149-153.

Sugawara, T., Lewén, A., Noshita, N., Gasche, Y. & Chan, P.H. (2002) Effects of global ischemia duration on neuronal, astroglial, oligodendroglial, and microglial reactions in the vulnerable hippocampal CA1 subregion in rats. *J. Neurotrauma*, **19**, 85-98.

Takeo, S., Niimura, M., Miyake-Takagi, K., Nagakura, A., Fukatsu, T., Ando, T., Takagi, N., Tanonaka, K. & Hara, J. (2003) A possible mechanism for improvement by a cognition-enhancer nefiracetam of spatial memory function and cAMP-mediated signal transduction system in sustained cerebral ischaemia in rats. *Br. J. Pharmacol.*, **138**, 642-654.

Tanaka, K., Hori, K., Wada-Tanaka, N., Nomura, M. & Ogawa, N. (2001) FK506 ameliorates the discrimination learning impairment due to preventing the rarefaction of white matter induced by chronic cerebral hypoperfusion in rats. *Brain Res.*, **906**, 184-189.

Tiwari, S.C., Srivastava, G., Tripathi, R.K., Pandey, N.M., Agarwal, G.G., Pandey, S. & Tiwari, S. (2013) Prevalence of psychiatric morbidity amongst the community dwelling rural older adults in northern India. *Indian J. Med. Res.*, **138**, 504-514.

White, B.C., Sullivan, J.M., DeGracia, D.J., O'Neil, B.J., Neumar, R.W., Grossman, L.I., Rafols, J.A. & Krause, G.S. (2000) Brain ischemia and reperfusion: molecular mechanisms of neuronal injury. *J. Neurol. Sci.*, **179**, 1-33.

Wu, Y.Y., Wu, W.Y., Gong, H.L., Li, W.Z. & Yin, Y.Y. (2014) Astragalosides attenuate learning and memory impairment in rats following ischemia-reperfusion injury. *Mol. Med. Rep.*, **9**, 1319-1324.

Xiao, Y., Wang, J., Jiang, S. & Luo, H. (2012) Hyperbaric oxygen therapy for vascular dementia. *Cochrane Database Syst. Rev.*, **7**, CD009425.

Zhang, Y., Cui, Y., Zhou, Z., Sha, J., Li, Y. & Liu, J. (2010a) Altered global gene expressions of human placentae subjected to assisted reproductive technology treatments. *Placenta*, **31**, 251-258.

Zhang, L.M., Jiang, C.X. & Liu, D.W. (2009) Hydrogen sulfide attenuates neuronal injury induced by vascular dementia via inhibiting apoptosis in rats. *Neurochem. Res.*, **34**, 1984-1992.

Zhang, Y., Xu, Y., Nie, H., Lei, T., Wu, Y., Zhang, L. & Zhang, M. (2012a) Prevalence of dementia and major dementia subtypes in the Chinese populations: a meta-analysis of dementia prevalence surveys, 1980-2010. *J. Clin. Neurosci.*, **19**, 1333-1337.

Zhang, T., Yang, Q.W., Wang, S.N., Wang, J.Z., Wang, Q., Wang, Y. & Luo, Y.J. (2010b) Hyperbaric oxygen therapy improves neurogenesis and brain blood supply in piriform cortex in rats with vascular dementia. *Brain Inj.*, **24**, 1350-1357.

Zhang, X.L., Zheng, S.L., Dong, F.R. & Wang, Z.M. (2012b) Nimodipine improves regional cerebral blood flow and suppresses inflammatory factors in the hippocampus of rats with vascular dementia. *J. Int. Med. Res.*, **40**, 1036-1045.

Zuliani, G., Guerra, G., Ranzini, M., Rossi, L., Munari, M.R., Zurlo, A., Blè, A., Volpato, S., Atti, A.R. & Fellin, R. (2007a) High interleukin-6 plasma levels are associated with functional impairment in older patients with vascular dementia. *Int. J. Geriatr. Psychiatry*, **22**, 305-311.

Zuliani, G., Ranzini, M., Guerra, G., Rossi, L., Munari, M.R., Zurlo, A., Volpato, S., Atti, A.R., Blè, A. & Fellin, R. (2007b) Plasma cytokines profile in older subjects with late onset Alzheimer's disease or vascular dementia. *J. Psychiatr. Res.*, **41**, 686-693.